SPATIO-TEMPORAL MODEL FOR CPUE STANDARDIZATION: APPLICATION TO BLUE MARLIN CAUGHT BY JAPANESE TUNA LONGLINE FISHERY IN THE INDIAN OCEAN FROM 1979 TO 2023

Mikihiko Kai[1]

SUMMARY

Abundance indices of blue marlin caught by Japanese tuna-longline fishery in the Indian Ocean were estimated using logbook data from 1979 to 2023. The nominal CPUEs were standardized using the spatio-temporal generalized linear mixed model (GLMM, sdmTMB) to update the annual changes in the abundance indices and to account for spatiotemporal changes in fishing locations resulting from shifts in target species, including tuna and tuna-like species. Since blue marlins are mainly distributed in the tropical and subtropical areas in the Indian Ocean, only data north of 30 °S was used. Due to the shrinkage of operational areas of Japanese longline fleets after 2010, calculations were performed separately for the periods 1979-2010 and 2011-2023. The predicted annual CPUEs between 1979 and 2010 revealed a declining trend from 1979 to 2001. Since then, the annual CPUEs have remained relatively stable, with no substantial fluctuations. The predicted annual CPUEs between 2011 and 2023 showed a decline until 2021 and exhibited an increasing trend from 2021 onward. The predicted CPUE using the spatio-temporal model with a large amount of data collected in the wide area in the Indian Ocean is very useful information about the spatiotemporal changes in the abundance. However, for estimates after 2010, due to reduced area coverage, careful consideration is required in cases where there are conflicts with annual CPUE trends in major fleets such as Chinese Taipei.

KEYWORDS

Blue marlin, Makaira mazara, Japanese tuna longline, CPUE standardization, GLMM, spatio-temporal model

1. Introduction

The blue marlin (*Makaira mazara*) is a highly migratory, cosmopolitan species found throughout the tropical and subtropical waters of the Pacific and Indian Oceans (Nakamura 1985). This species is classified as epipelagic and oceanic, predominantly inhabiting regions where the sea surface temperature exceeds 24 °C. Its distribution is closely associated with thermal boundaries, and it exhibits pronounced seasonal latitudinal migrations in response to changes in oceanographic conditions.

The benchmark stock assessment for the blue marlins in the Indian Ocean was conducted in 2022 using stock synthesis (SS3) model (Xu et al. 2022) and Just Another Bayesian Biomass Assessment (JABBA) model with fishery data for 1950-2020 (Parker and Kerwath 2022). The models indicated that the stock was currently overfished and subject to overfishing when using maximum sustainable yield as the management reference point.

In the previous benchmark stock assessment in 2022, Japan provided standardized CPUEs (catch per unit effort) of blue marlin caught by Japanese tuna longline fishery operating in the Indian Ocean from 1979 to 2021. The annual CPUEs were estimated using generalized linear mixed model (GLMM, glmmTMB: Brooks *et al*. 2017) assuming a zero-inflated Poisson model with logbook data collected from Japanese commercial tuna longline fishery (Matsumoto *et al*. 2022). The model included year, season, and gear configuration (number of hooks between floats: hbf) as fixed effect, and the effects of area and vessel were given as random effects. The gear configuration was classified into shallow-set (hbf < 15) and deep-set (nhbf ≥ 15) in consideration of the change in

[1] Fisheries Resources Institute, Japan Fishery Research and Education Agency. 2-12-4, Fukuura Kanazawa, Yokohama, Kanagawa, Japan.

target fish species. The area was separated into three core areas (Northwest, Southwest, and Central east) with high catch of blue marlin following the approach by Yokoi et al. (2016) (**Fig. 1**). Overall, the annual changes in the standardized CPUEs showed a decreasing trend.

In the previous analysis, glmmTMB was used (Matsumoto *et al*. 2022), however the model lacks functionality for explicitly modeling spatial correlation structures. Recently, spatiotemporal statistical GLMM models such as INLA (Rue *et al*. 2009), VAST (Thorson 2019), and sdmTMB (Anderson *et al*. 2022) have been used to standardize the CPUE of tuna and tuna-like species. Among these, sdmTMB, which is an R package designed for spatiotemporal modeling using Template Model Builder (TMB), is the newest and has advantages on several aspects such as user-friendly interface and fast estimation.

The objective of this working paper is to estimate the standardized CPUE of blue marlin caught by Japanese tuna longline fishery operating in the Indian Ocean from 1979 to 2023 using spatio-temporal GLMM (sdmTMB) in consideration of spatial and temporal changes in the density.

2. Materials and Methods

2.1 Data sources

Set-by-set logbook data from Japanese tuna longline fisheries in the Indian Ocean was used to estimate the annual standardized CPUEs of blue marlins in the area from 1979 to 2023. The starting year is the same as the indices used in the last stock assessment in 2022. The logbook data includes information about date of operation, catch number of tuna and tuna-like species, amount of effort (number of hooks), hbf as a proxy for gear configuration, location/station (longitude and latitude) of set by resolution of 1 × 1 degree square, and vessel identity (vessel name).

2.2 Data filtering and separation

The logbook data in the Indian Ocean were filtered to remove inappropriate data and separated into categorical datasets for appropriate analysis.

1. Based on the dataset defined as pertaining to the Indian Ocean, set-by-set data from regions outside the Indian Ocean were excluded.
2. Set-by-set data prior to 1979 were excluded to maintain consistency with the previous analysis.
3. Set-by-set data entries with 'NA' for the blue marlin catch number were excluded.
4. Set-by-set data south of 30°S were excluded, as this region does not represent a major distribution area for blue marlin.
5. Set-by-set data with the number of hooks between floats (HBF) outside the range of 3 to 25 were excluded.
6. Set-by-set data from vessels with a total blue marlin catch of zero across all operations were excluded.
7. Set-by-set data from cruises with a total blue marlin catch of zero across all operations were excluded.
8. Create a set-by-set dataset in which both catch number and fishing effort are pooled by 1 x 1 grid so that all explanatory variables used in CPUE standardization do not overlap.
9. Set-by-set data were divided into two periods from1979 to 2010 and from 2011 to 2023 due to the contraction of operational areas of Japanese longline fleets after 2010 (see **Fig. 2**).

2.3 Catchability covariate

The nominal CPUEs of blue marlins were substantially influenced by year, quarter, vessel, number of hbf, and target change (**Fig. A1**). In the Indian Ocean, Japanese tuna longline fisheries change the target species by altering the operational area, gear configuration, season, etc. (**Fig. A2**). The number of hbf (**Fig. A3**) is commonly used to identify target change through changes in the depth of hook distribution (Bigelow et al. 2006). Cluster analysis based on k-means clustering of observed catch proportions for yellowfin tuna, bigeye tuna, and albacore (Carvalho et al. 2010; Chang et al. 2011) was also used to identify target species (**Fig. A4**). The issue of multicollinearity was evaluated using correlations among quarters, number of hbf, location, and cluster (**Fig. A5**). There were no strong correlations between each effect. Vessel name was treated as a random effect to account for individual differences in vessel catchability.

2.4 CPUE standardization with spatio-temporal model

The sdmTMB model (Anderson *et al*. 2022) can be written as

$$E[y_{s,t}] = \mu_{s,t},$$
$$\mu_{s,t} = f^{-1}(\mathrm{X}_{s,t}\boldsymbol{\beta} + O_{s,t} + \alpha_g + \omega_s + \epsilon_{s,t}), \quad (1)$$

where $y_{s,t}$ represents the response data (catch number of blue marlins) at station s (knot) and time t (year); μ represents the mean; f represents a link function (log); **X** represents design matrices of main effects; $\boldsymbol{\beta}$ represents a vector of fixed-effect coefficients (year, season, hbf, and cluster); O represents an offset (log-transformed number of hooks); α_g represents random intercept by group g (vessel names): ω_s represents a spatial component (a random field) : $\epsilon_{s,t}$ represents a spatiotemporal component (a random field).

To account for count-data of blue marlins with over-dispersion and moderate zero catch ratio (**Table 1**), two observation models (Poisson and Negative binomial models with a log function) were used.

The sdmTMB (version sdmTMB_0_6_0) software package for R (Anderson *et al.* 2022) was applied to standardize the nominal CPUE of blue marlins in the Indian Ocean from 1979 to 2023. The annual abundance index relative to the average $\hat{I}$ was estimated as:

$$\hat{I}(t) = \sum_{s=1}^{n_s}(E[y_{s,t}])/\{\sum_{t=1}^{n_t}\sum_{s=1}^{n_s}E[y_{s,t}]\}, \quad (2)$$

where n_s is total number of knots. One hundred knots were given in consideration of the computational cost and spatial density (**Fig. A6**).

The 95 % confidence intervals were calculated using the standard error estimated from the generalized delta method in TMB.

2.5 Model selection and diagnostics

Model selection was conducted in two stages. First, the two observation models were compared using the full model structure. Next, the optimal model structure was compared by sequentially adding explanatory variables to the simple null model (Model-0). The best model was selected using AIC (Akaike 1973) and BIC (Schwarz 1978) for both stages. For the best model, the goodness of fit was examined using residual plot for each explanatory variable and QQ plot. The residuals were computed using a simulation-based approach to create scaled residuals for GLMM in package R (DHARMa), which uses a randomized quantile (Dunn and Smyth 1996) to produce continuous normal residuals.

3. Results

3.1 Summary of data filtering and basic annual trends

The data filtering based on the year of catch, number of hbf, catch number of blue marlin, and operational area reduced the number of records for this analysis from 1,740,919 sets to 206,480 sets. Annual catch numbers, number of hooks, nominal CPUE, and positive catch ratio for this species before and after data filtering are shown in **Fig. 3**. Annual catches of blue marlins were slightly changed, but the annual trends were almost the same before and after data filtering. The annual catch number showed a sharp increasing trend after 1979, reaching a peak of approximately 20,000 fish per year in 1983. However, it declined rapidly between 1985 and 1989. Although there was an increase in the late 1990s and late 2000s, the annual catch has remained below 5,000 fish since 2010, showing a gradual downward trend. The levels of annual fishing effort, annual nominal CPUE, and annual positive catch ratio significantly changed after data filtering. The actual fishing effort remained relatively high, with fluctuations, until around 2009, but declined sharply after 2010. Due to data filtering, many records that did not include catches of blue marlin were removed, resulting in a noticeable decrease in effort, especially during the period from 1979 to the early 2000s. After filtering data, both CPUE and the positive catch ratio increased significantly across all years. The nominal CPUE exhibited a gradual downward trend from 1979 to 2023. In contrast, the positive catch ratio has shown a slight declining trend since 1980.

3.2 Selection of the best model

All models converged reasonably well, with a positive definite Hessian matrix and a small maximum gradient (< 0.0001) (**Tables 2 and 3**). The negative binomial model was selected as the most parsimonious model in the first-stage model selection for both periods (**Table 2**). Subsequently, Model-6 and Model-4 were selected as the most parsimonious models in the second-stage model selection for both periods, respectively (**Table 3**). Differences in the observation model and model structure did not significantly affect the overall trend (**Figs. 4 and 5**). A list of all parameters and estimates for the best models is provided in **Table 4**.

3.3 Annual trends in CPUE

The predicted CPUE exhibited a gradual overall decline, with the exception of a relatively stable trend observed after 2000 (**Fig. 6**). The predicted annual CPUEs between 1979 and 2010 revealed a declining trend from 1979 to 2001. Since then, the annual CPUEs have remained relatively stable, with no substantial fluctuations. The predicted annual CPUEs between 2011 and 2023 showed a decline until 2021 and exhibited an increasing trend from 2021 onward. One possible reason for the wide 95% confidence intervals of CPUE from 1979 to 2010 is the significant fluctuations in catch number and fishing effort during this period, as well as substantial changes in fishing areas from year to year. In contrast, since 2011, both catch number and fishing effort have remained low and stable, which likely contributed to narrower confidence intervals.

3.4 Model diagnostics

Diagnostic plots of goodness-of-fit for the best models (Model-6 and Model-4) didn't show a serious deviation from normality and model misspecification (**Figs. 7 and 8**). These results suggested that the fittings of the best model to the data were good.

3.5 Spatial maps of estimated CPUE

The spatial maps of predicted CPUEs for the former period from 1979 to 2010 clearly showed higher CPUEs of blue marlin in the tropical water between 10°S and 10°N throughout the years (**Fig. 9**). However, the spatial maps of predicted CPUEs for the latter period from 2011 to 2023 exhibited higher CPUEs of blue marlin in the coastal areas of offshore waters of southeastern Africa in addition to the tropical waters (**Fig. 10**).

4. Discussions

This paper predicted the historical trend in abundance indices of blue marlins caught by the Japanese tuna longline fishery in the Indian Ocean from 1979 to 2023 to provide the abundance indices for the upcoming benchmark stock assessment in 2025. Although the zero-inflated Poisson model was used in the previous analysis (Matsumoto et al. 2022), a negative binomial model was used in the present analysis. Given that the datasets after data filtering exhibit a moderate zero catch ratio and a variance significantly greater than the mean (see **Table 1**), the negative binomial model is considered appropriate.

The CPUE trend observed in this study is similar to the previously reported declining trend, indicating that blue marlin has historically been overexploited and its stock has decreased. The reason why the coefficient of variation (CV) of the abundance index is smaller in the latter period than in the former is likely due to greater year-to-year variation in fishing locations during the earlier period from 1979 to 2010, which reduced the estimation precision.

In the previous CPUE analysis, standardization was conducted using three core areas. However, as shown in **Fig. 1**, these areas are unlikely to represent CPUE trends across the entire Indian Ocean. Therefore, using data north of 30°S, as done in the present study, is considered a more appropriate approach for estimating the abundance index. Additionally, in the previous CPUE standardization, CPUE in the northwestern Indian Ocean was not estimated after 2011. This issue was resolved in the present study by dividing the data into two-time blocks.

Even though the fishing effort (number of hooks) in logbook records has been decreasing annually (**Fig. A7**), the method presented here may be more suitable for representing the overall abundance index in the Indian Ocean for the time being, as spatiotemporal model can predict the missing data regarding particular year and area using the correlations.

We recommend using the predicted annual CPUEs of blue marlins caught by Japanese tuna longline fishery in the Indian Ocean from 1979 to 2023 as a representative of abundance indices in the Indian Ocean due to a wide coverage of the main distributional areas (tropical and subtropical waters) of blue marlins over time, sufficient long time series of data, and statistical soundness of the spatiotemporal model. However, for estimates after 2010, due to reduced area coverage, careful consideration is required in cases where there are conflicts with annual CPUE trends in major fleets such as Chinese Taipei.

References

Akaike, H. 1973. Information theory and an extension of the maximum likelihood principle. *In* Petrov, B.N., Csaki, F. (Eds.) Second International Symposium on Information Theory, Budapest, Akademiai Kiado, pp 267–281.

Anderson, S.C., Ward, E.J., English, P.A., Barnett, L.A.K., and Thorson, J.T. 2022. sdmTMB: An R Package for Fast, Flexible, and User-Friendly Generalized Linear Mixed Effects Models with Spatial and Spatiotemporal Random Fields.
bioRxiv 2022.03.24.485545; doi: https://doi.org/10.1101/2022.03.24.485545

Bigelow, K. Musyl, M.K. Poisson, F. and Kleiber, P. 2006. Pelagic longline gear depth and shoaling. Fish. Res. 77: 173–183. https://doi.org/10.1016/j.fishres.2005.10.010

Brooks, ME., Kristensen, K., van Benthem, KJ., Magnusson, A., Berg, CW., Nielsen, A., Skaug, HJ., M .achler, M., Bolker, B,M. 2017 Modeling zeroachler, M., Bolker, B,M. 2017 Modeling zero-inflated count data with inflated count data with glmmTMB. bioRxiv preprint first posted online. pp 14.

Carvalho, F.C. Murie, D.J. Hazin, F.H.V. Hazin, H.G. Leite-mourato, B. Travassos, P. and Burgess, G.H. 2010. Catch rates and size composition of blue sharks (*Prionace glauca*) caught by the Brazilian pelagic longline fleet in the southwestern Atlantic Ocean. Aquat. Living Resour. 23: 373–385. https://doi.org/10.1051/alr/2011005

Chang, S.K. Hoyle, S. and Liu, H.I. 2011. Catch rate standardization for yellowfin tuna (*Thunnus albacares*) in Taiwan's distant-water longline fishery in the Western and Central Pacific Ocean, with consideration of target change. Fish. Res. 107(1-3): 210–220. https://doi.org/10.1016/j.fishres.2010.11.004

Dunn, K. P., and Smyth, G. K., 1996. Randomized quantile residuals. J. Comput. Graph. Stat. 5, 236-244.

Matsumoto, T., Taki, K., and Ijima, H. 2022. Standardized CPUE of blue marlin (*Makaira mazara*) caught by by Japanese longline fishery in the Indian Ocean: Analysis between 1979 and 2021. IOTC-2022-WPB20-10

Nakamura, H. 1985. FAO species catalogue. Vol.5. Billfishes of the world. ac480e06.pdf

Parker, D., and Kerwath, S. 2022. Updated stock assessment of blue marlin (Makaira nigricans) in the Indian Ocean using JABBA. IOTC-2022-WPB20-12.

Rue, H., Martino, S., and Chopin, N. 2009. Approximate Bayesian inference for latent Gaussian models by using integrated nested Laplace approximations. Journal of the Royal Statistical Society: Series B (Statistical Methodology), 71(2), 319-392.

Schwarz, G. 1978. Estimating the dimension of a model. Ann. Stat. 6(2): 461–464.

Thorson, J.T. 2019. Guidance for decisions using the Vector Autoregressive Spatio-Temporal (VAST) package in stock, ecosystem, habitat and climate assessments. Fish. Res. 210, 143−161.

Xu, W. Q., Wang, S. P., and Lin, C. Y. 2022. Stock assessment of blue marlin (Makaira nigricans) in the Indian Ocean using Stock Synthesis. IOTC-2022-WPB-13 rev1.

Yokoi, H., Semba, Y., Satoh, K., and Nishida, T. 2016. Standardization of catch rate for blue marlin (Makaira mazara) exploited by the Japanese tuna longline fisheries in the Indian Ocean from 1971 to 2015. IOTC-2016-WPB14-22.

Table 1. Summary of dispersion ratio, percentage of zero catch, and sample number used in the model for blue marlins in the Indian Ocean from 1979 to 2023.

Table 2. Summary of structures and outputs for different observation models for blue marlins in the Indian Ocean for the former period (1997-2010) and latter period (2011-2023). "Δ" denotes a difference between the value of criteria and the minimum value.

Table 3. Summary of structures and outputs for different model structures for blue marlins in the Indian Ocean for the former period (1997-2010) and latter period (2011-2023). "Δ" denotes a difference between the value of criteria and the minimum value.

Table 1. Summary of dispersion ratio, percentage of zero catch, and sample number used in the model for blue marlins in the Indian Ocean from 1979 to 2023.

Year	Dispersion ratio	Percentage of zero catch	sample number (×1000)	Year	Dispersion ratio	Percentage of zero catch	sample number (×1000)
1979	62.6	35	2,239	2001	5.6	60	4,958
1980	19.7	29	2,974	2002	4.8	64	6,655
1981	7.4	33	4,509	2003	5.1	63	4,905
1982	9.0	31	5,180	2004	5.9	60	5,206
1983	8.5	28	6,364	2005	3.9	61	6,071
1984	7.5	28	5,700	2006	4.9	57	8,630
1985	7.1	28	7,002	2007	3.9	58	9,163
1986	8.0	33	6,841	2008	5.3	61	7,229
1987	6.1	31	5,037	2009	5.1	62	6,273
1988	5.0	36	4,668	2010	7.3	62	2,884
1989	7.6	45	2,720	2011	11.2	47	1,449
1990	5.1	45	2,930	2012	5.7	54	2,037
1991	4.7	48	2,149	2013	6.0	59	1,928
1992	9.0	45	1,567	2014	5.1	62	2,036
1993	6.2	47	1,854	2015	4.8	62	1,623
1994	9.4	48	2,742	2016	8.0	67	1,455
1995	9.9	55	3,078	2017	11.5	64	1,515
1996	10.4	58	4,368	2018	8.2	68	1,486
1997	13.0	44	6,382	2019	4.8	68	1,341
1998	6.1	44	7,561	2020	5.2	72	1,297
1999	6.9	49	6,088	2021	4.2	75	1,403
2000	7.2	48	6,467	2022	4.3	73	1,233
				2023	7.1	61	1,020

Table 2. Summary of structures and outputs for different observation models for blue marlins in the Indian Ocean for the former period (1997-2010) and latter period (2011-2023). "Δ" denotes a difference between the value of criteria and the minimum value.

1979-2010

Model	Observation model	Number of parameters	AIC	ΔAIC	BIC	ΔBIC	Maximum gradient
1	Poisson	44	510,988	46,582	511,427	46,572	< 0.0001
2	Negative binomial	45	464,406	0	464,855	0	< 0.0001

2011-2023

Model	Observation model	Number of parameters	AIC	ΔAIC	BIC	ΔBIC	Maximum gradient
1	Poisson	25	40,937	1,459	41,134	1,451	< 0.0001
2	Negative binomial	26	39,478	0	39,683	0	< 0.0001

Table 3. Summary of structures and outputs for different model structures for blue marlins in the Indian Ocean for the former period (1997-2010) and latter period (2011-2023). "Δ" denotes a difference between the value of criteria and the minimum value.

1979-2010

Model	Catch rate predictors of random effect	Number of parameters	AIC	ΔAIC	BIC	ΔBIC	Maximum gradient
0	Year	33	505524	41118	505853	40998	< 0.0001
1	Year + Station	37	480305	15899	480674	15819	< 0.0001
2	Year + Station + Year and Station	38	472246	7840	472626	7770	< 0.0001
3	Year + Station + Year and Station + Vessel	39	465455	1049	465844	989	< 0.0001
4	Year + Station + Year and Station + Vessel + Season	42	464852	446	465272	416	< 0.0001
5	Year + Station + Year and Station + Vessel + Season + Cluster	43	464851	445	465280	425	< 0.0001
6	Year + Station + Year and Station + Vessel + Season + HBF + Cluster	45	464406	0	464855	0	< 0.0001

2011-2023

Model	Catch rate predictors of random effect	Number of parameters	AIC	ΔAIC	BIC	ΔBIC	Maximum gradient
0	Year	14	43836	4359	43947	4285	< 0.0001
1	Year + Station	18	40350	872	40492	831	< 0.0001
2	Year + Station + Year and Station	19	40067	590	40217	556	< 0.0001
3	Year + Station + Year and Station + Vessel	20	39640	162	39798	136	< 0.0001
4	Year + Station + Year and Station + Vessel + Season	23	39480	2	39662	0	< 0.0001
5	Year + Station + Year and Station + Vessel + Season + Cluster	24	39480	3	39670	8	< 0.0001
6	Year + Station + Year and Station + Vessel + Season + HBF + Cluster	26	39478	0	39683	21	< 0.0001

Table 4. List of all parameters and estimates of the selected models (Model-4 and Model-6) for blue marlins in the Indian Ocean for the former period (1997-2010) and latter period (2011-2023).

1979-2010

No	Parameter name	Symbol	Type	Estimates
1	Spatial decorrelation rate	κ	Fixed	0.203
2	Dispersion parameter of negative binomial model	φ	Fixed	2.02
3	Northings anisotropy	h_1	Fixed	1.21
4	Anisotropic correlation	h_2	Fixed	0.98
5	Spatial random field marginal variance	$\sigma_{\omega 2}$	Fixed	1.85
6	Spatiotemporal random field marginal variance	$\sigma_{\epsilon 2}$	Fixed	2.37
7	Coefficient of year, three month quarter, hbbf, and cluster	β	Fixed	Not shown
8	IID random intercept deviation for group g	α_g	Random	Not shown
9	Spatial random field at point *s* (knot)	ω_s	Random	Not shown
10	Spatiotemporal random field at point *s* and time *t* (knot)	$\varepsilon_{s,t}$	Random	Not shown

2011-2023

No	Parameter name	Symbol	Type	Estimates
1	Spatial decorrelation rate	κ	Fixed	0.212
2	Dispersion parameter of negative binomial model	φ	Fixed	3.05
3	Northings anisotropy	h_1	Fixed	0.95
4	Anisotropic correlation	h_2	Fixed	0.90
5	Spatial random field marginal variance	$\sigma_{\omega 2}$	Fixed	1.69
6	Spatiotemporal random field marginal variance	$\sigma_{\epsilon 2}$	Fixed	3.39
7	Coefficient of year, three month quarter, hbf, and cluster	β	Fixed	Not shown
8	IID random intercept deviation for group g	α_g	Random	Not shown
9	Spatial random field at point *s* (knot)	ω_s	Random	Not shown
10	Spatiotemporal random field at point *s* and time *t* (knot)	$\varepsilon_{s,t}$	Random	Not shown

Table 5. Summary of annual CPUE predicted by spatio-temporal model along with corresponding estimates of the coefficient of variations (CV), annual nominal CPUE for blue marlins, and number of hooks in the Indian Ocean from 1979 to 2023. Values are predicted from the best fitting models (Model-4 and Model-6) for the former period (1997-2010) and latter period (2011-2023), and CPUEs are scaled by average CPUE.

Year	Predicted CPUE	Nominal CPUE	CV	Number of hooks (mil.)
1979	2.41	2.15	0.15	9.71
1980	2.10	2.11	0.15	13.23
1981	1.69	1.79	0.14	20.42
1982	1.78	1.95	0.14	25.54
1983	1.93	2.12	0.14	32.16
1984	1.94	1.94	0.14	29.31
1985	1.69	1.81	0.14	36.88
1986	1.46	1.61	0.14	34.95
1987	1.48	1.51	0.14	26.79
1988	1.25	1.29	0.14	24.11
1989	1.02	1.01	0.15	14.35
1990	0.87	0.83	0.15	17.34
1991	0.86	0.77	0.15	12.76
1992	1.28	0.93	0.15	10.15
1993	1.11	0.88	0.15	12.43
1994	1.18	1.04	0.15	20.68
1995	0.70	0.66	0.15	25.87
1996	0.62	0.61	0.14	37.22
1997	0.87	0.91	0.14	51.99
1998	0.80	0.87	0.14	54.74
1999	0.68	0.69	0.14	46.00
2000	0.64	0.72	0.14	50.98
2001	0.42	0.40	0.14	43.67
2002	0.35	0.34	0.14	55.44
2003	0.35	0.34	0.15	40.08
2004	0.38	0.40	0.14	42.10
2005	0.33	0.35	0.14	51.57
2006	0.36	0.41	0.14	72.87
2007	0.33	0.39	0.14	75.57
2008	0.34	0.39	0.14	60.90
2009	0.29	0.37	0.14	47.88
2010	0.50	0.43	0.16	23.28

Year	Predicted CPUE	Nominal CPUE	CV	Number of hooks (mil.)
2011	1.80	1.80	0.06	17.21
2012	1.32	1.43	0.04	19.78
2013	1.16	1.16	0.05	19.40
2014	0.96	1.00	0.05	20.42
2015	1.02	0.99	0.05	16.89
2016	0.80	0.88	0.05	15.85
2017	1.08	1.14	0.05	15.48
2018	0.90	0.93	0.06	14.82
2019	0.73	0.69	0.06	13.76
2020	0.74	0.61	0.07	13.26
2021	0.52	0.52	0.07	13.05
2022	0.73	0.62	0.08	10.15
2023	1.23	1.23	0.08	9.65

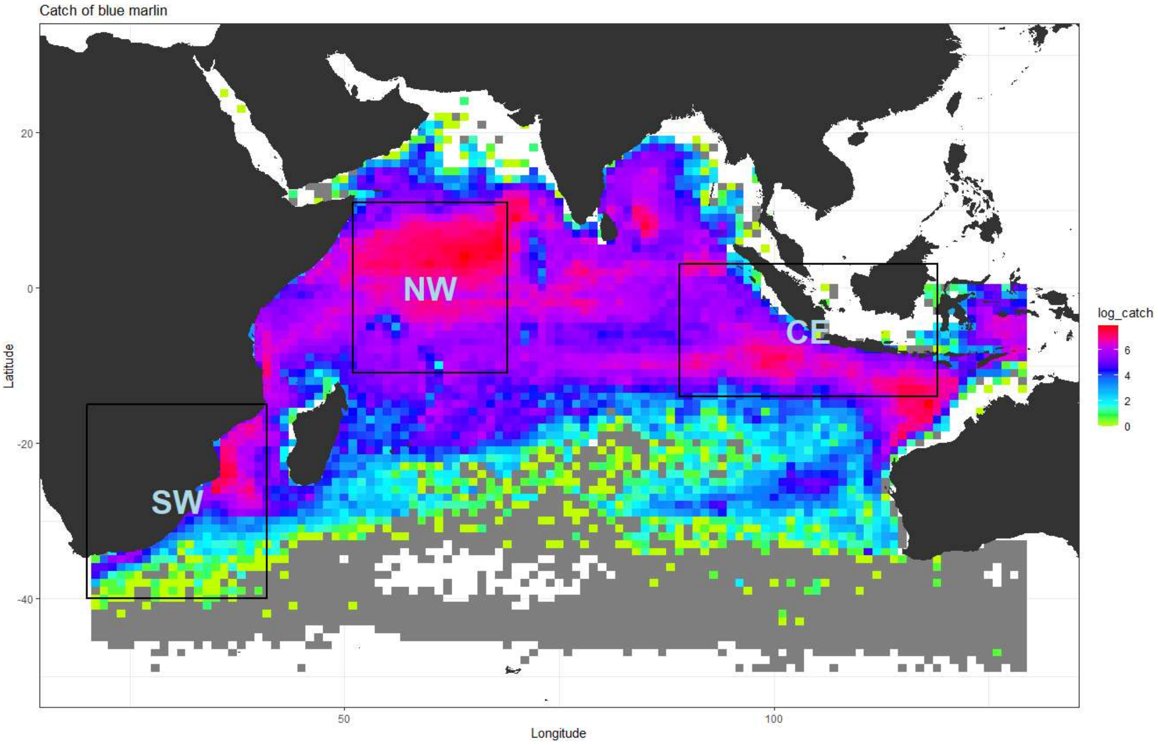

Fig. 1 Spatial distribution of blue marlines caught by Japanese longline fleets operated in the Indian Ocean from 1952 to 2023. The three areas (SW, NW, CE) represent the core distribution waters of blue marlin used in the previous CPUE standardization.

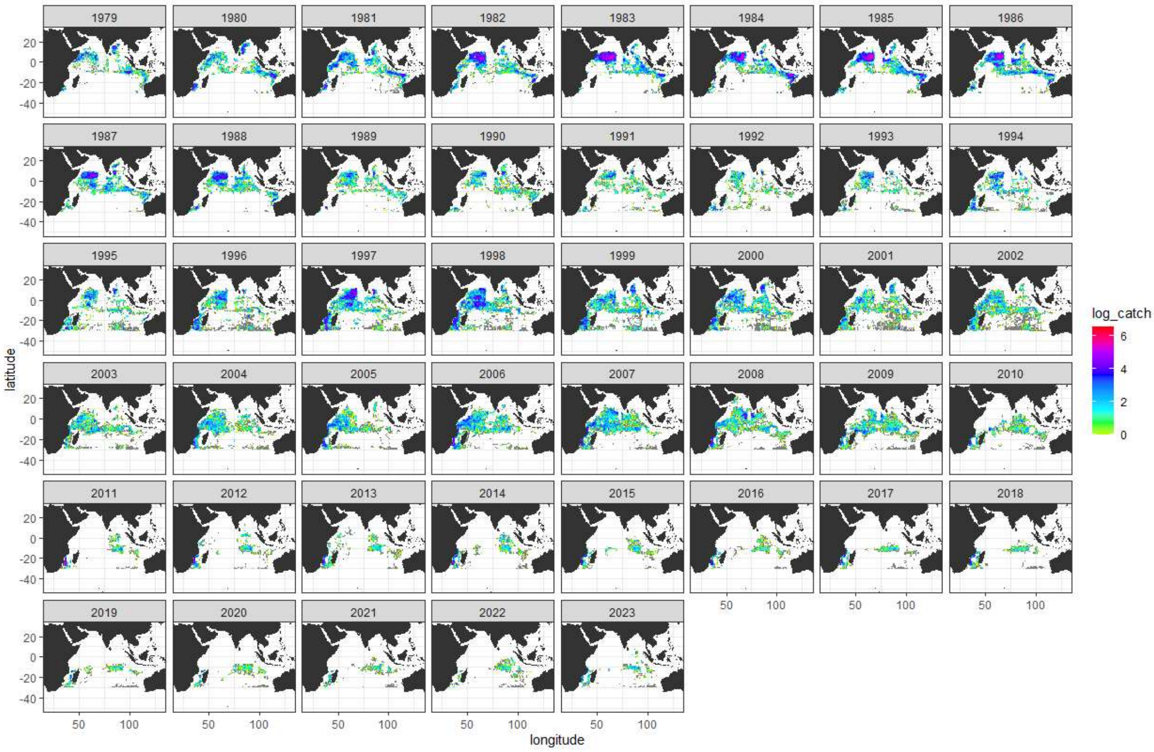

Fig. 2 Spatiotemporal changes in the log-transformed catch number of blue marlines based on logbook data of Japanese longline fleets operated in the Indian Ocean from 1979 to 2023. The data south of 30 °S was excluded, as this region does not represent a major distribution area for blue marlin.

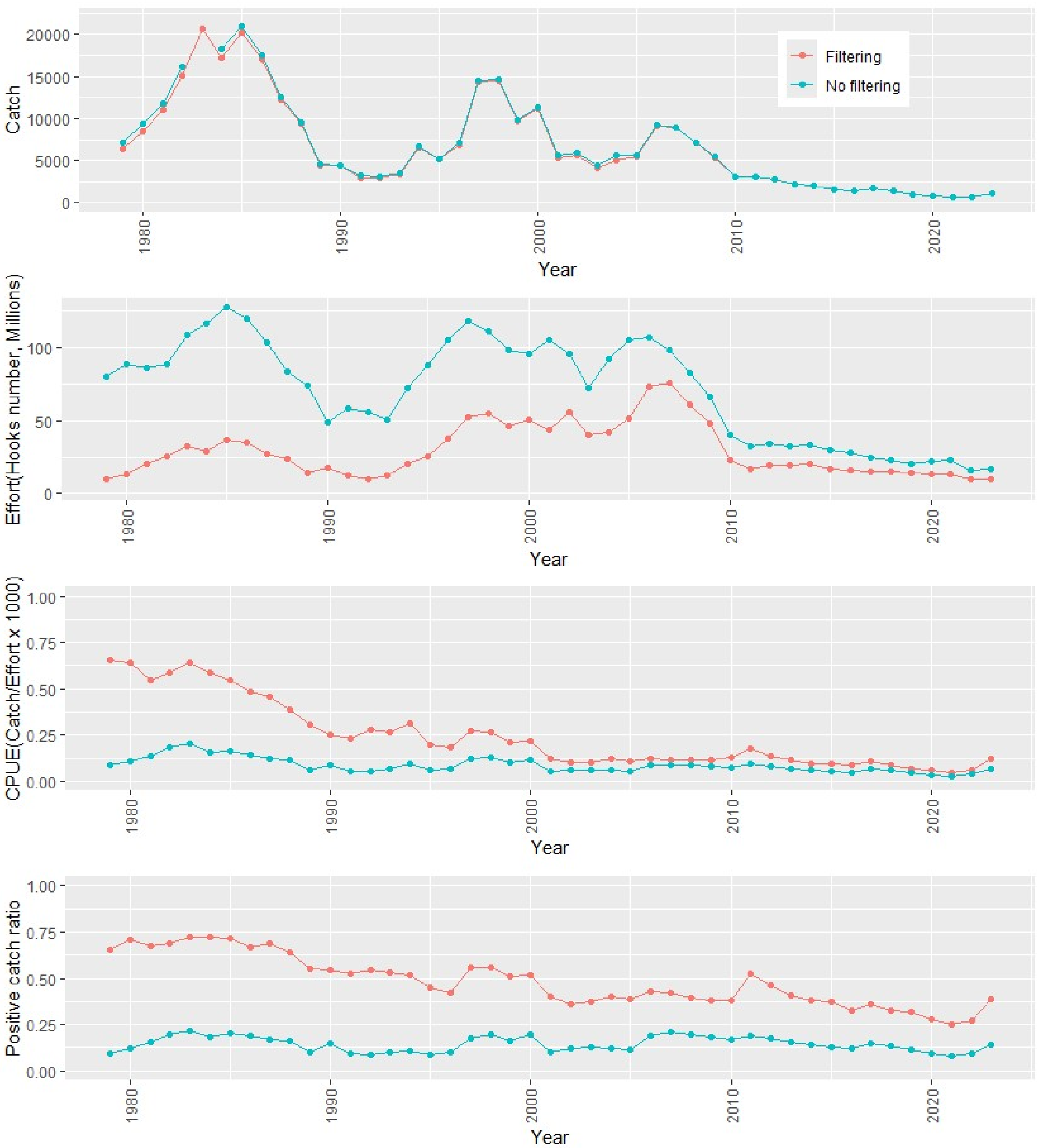

Fig. 3 Annual catch in numbers, number of hooks (millions), nominal CPUE (per 1000 hooks), and positive catch ratio for blue marlins in the Indian Ocean before and after data filtering from 1979 to 2023.

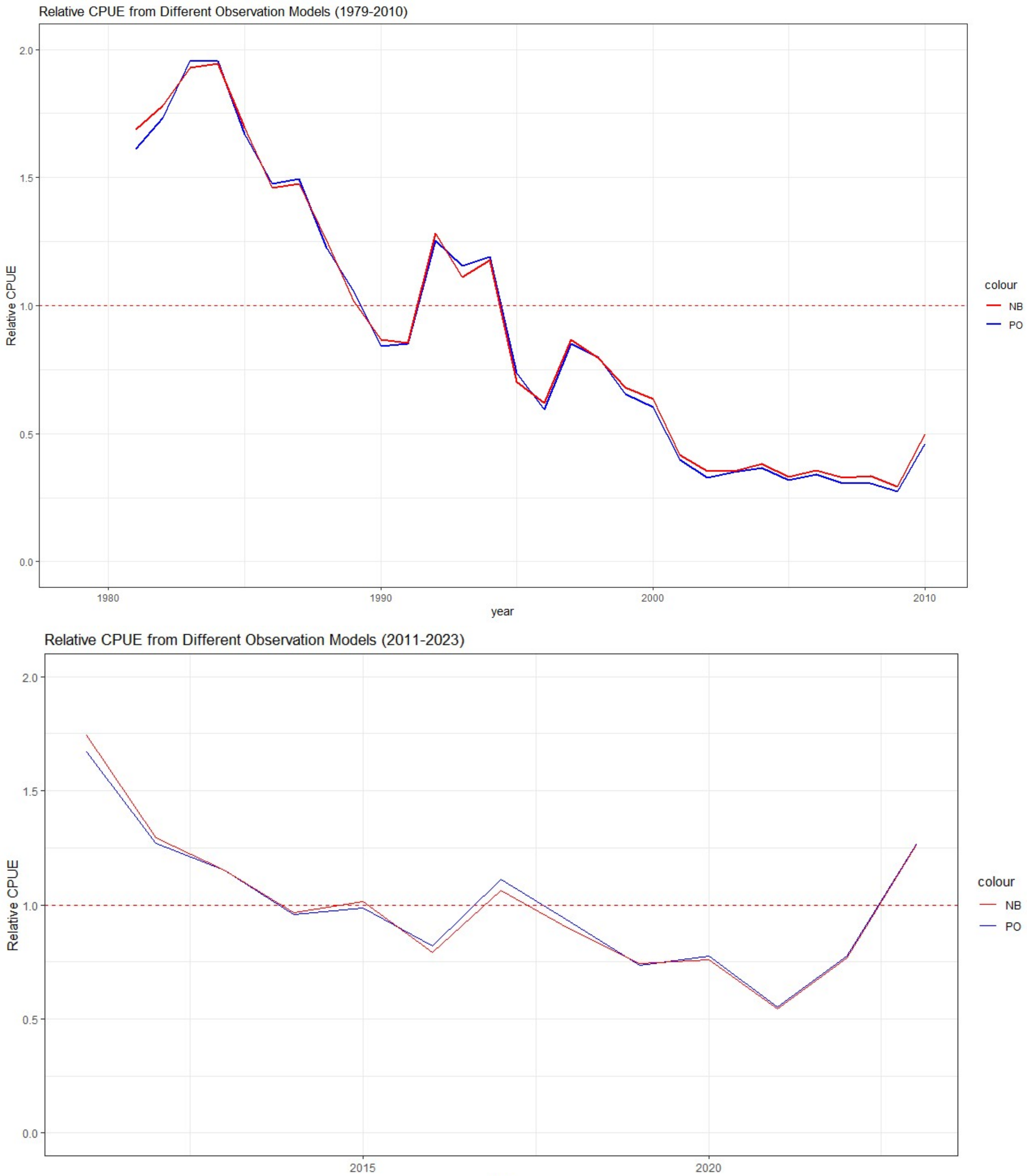

Fig. 4 Comparisons of predicted annual CPUE relative to its average among different observation models for the former period (1979-2010) and latter period (2011-2023). For details of the models, see **Table 2**. Horizontal red broken line denotes mean of relative values (1.0)

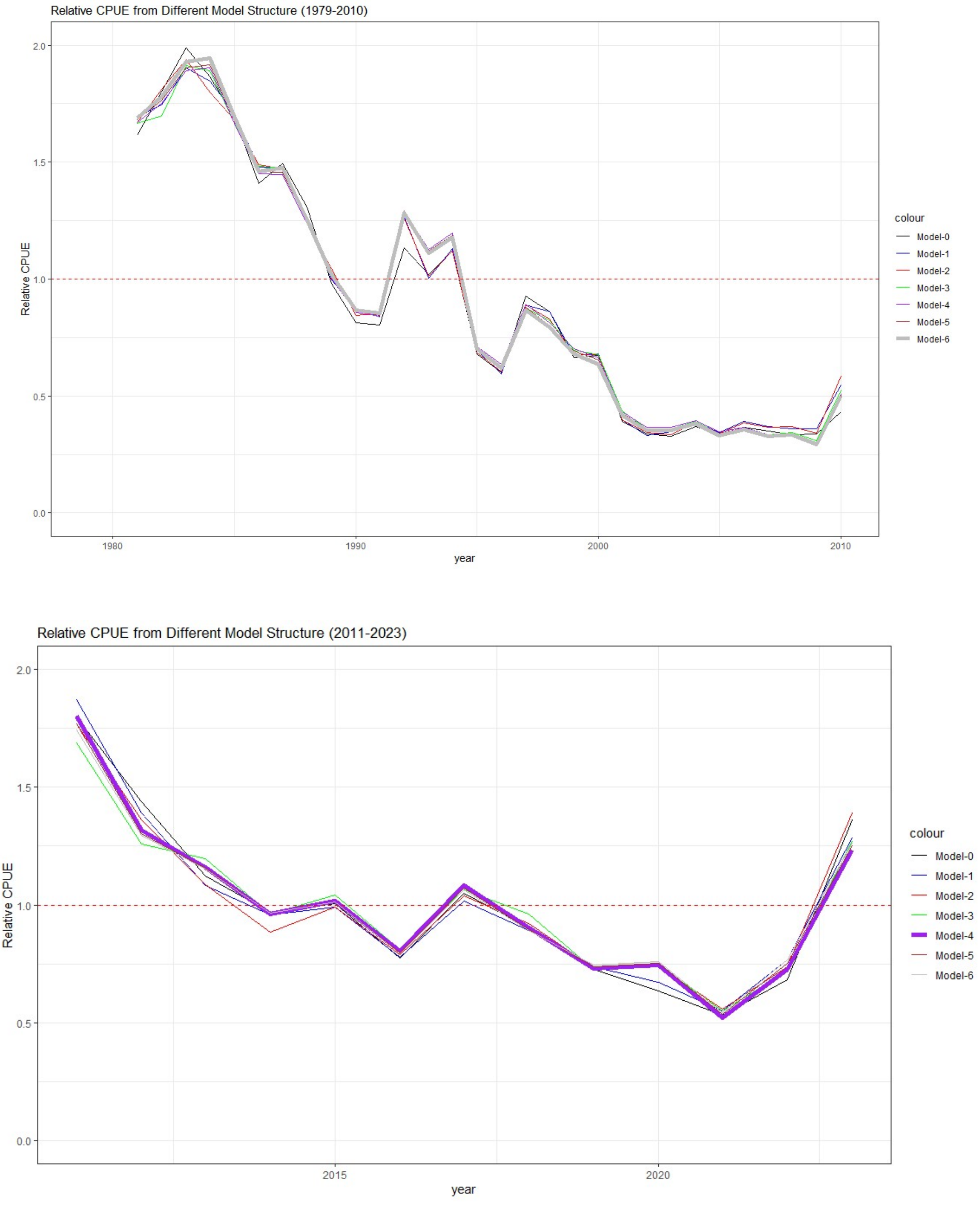

Fig. 5 Comparisons of predicted annual CPUE relative to its average among different model structures (lower panels) for the former period (1979-2010) and latter period (2011-2023). For details of the models, see **Table 3**. Horizontal red broken line denotes mean of relative values (1.0)

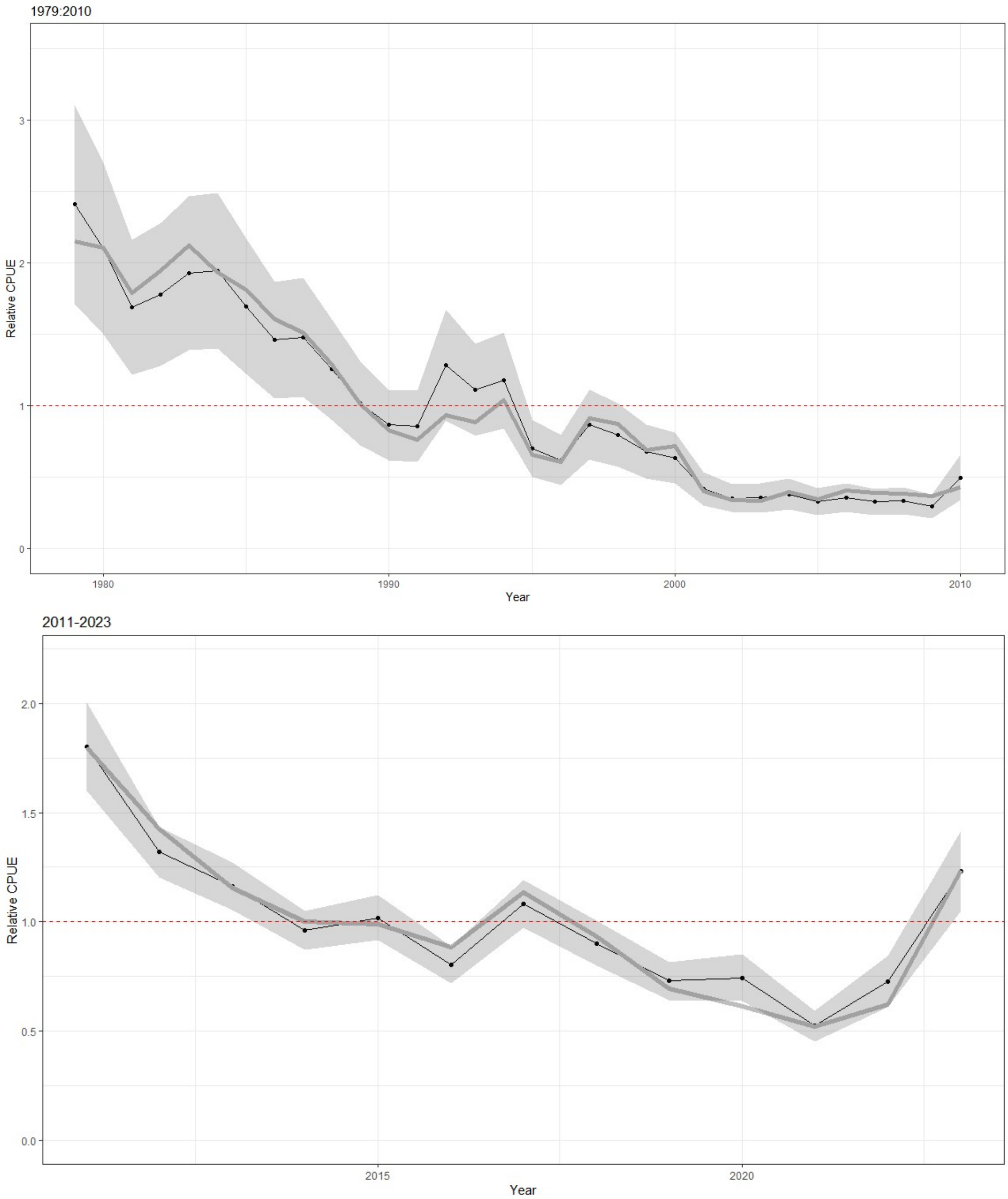

Fig. 6 Annual predicted CPUE relative to its average for the former period (1979-2010) and latter period (2011-2023). Gray solid line denotes nominal CPUE relative to its average, shadow denotes 95% confidence intervals, and horizontal red broken line denotes mean of relative values (1.0).

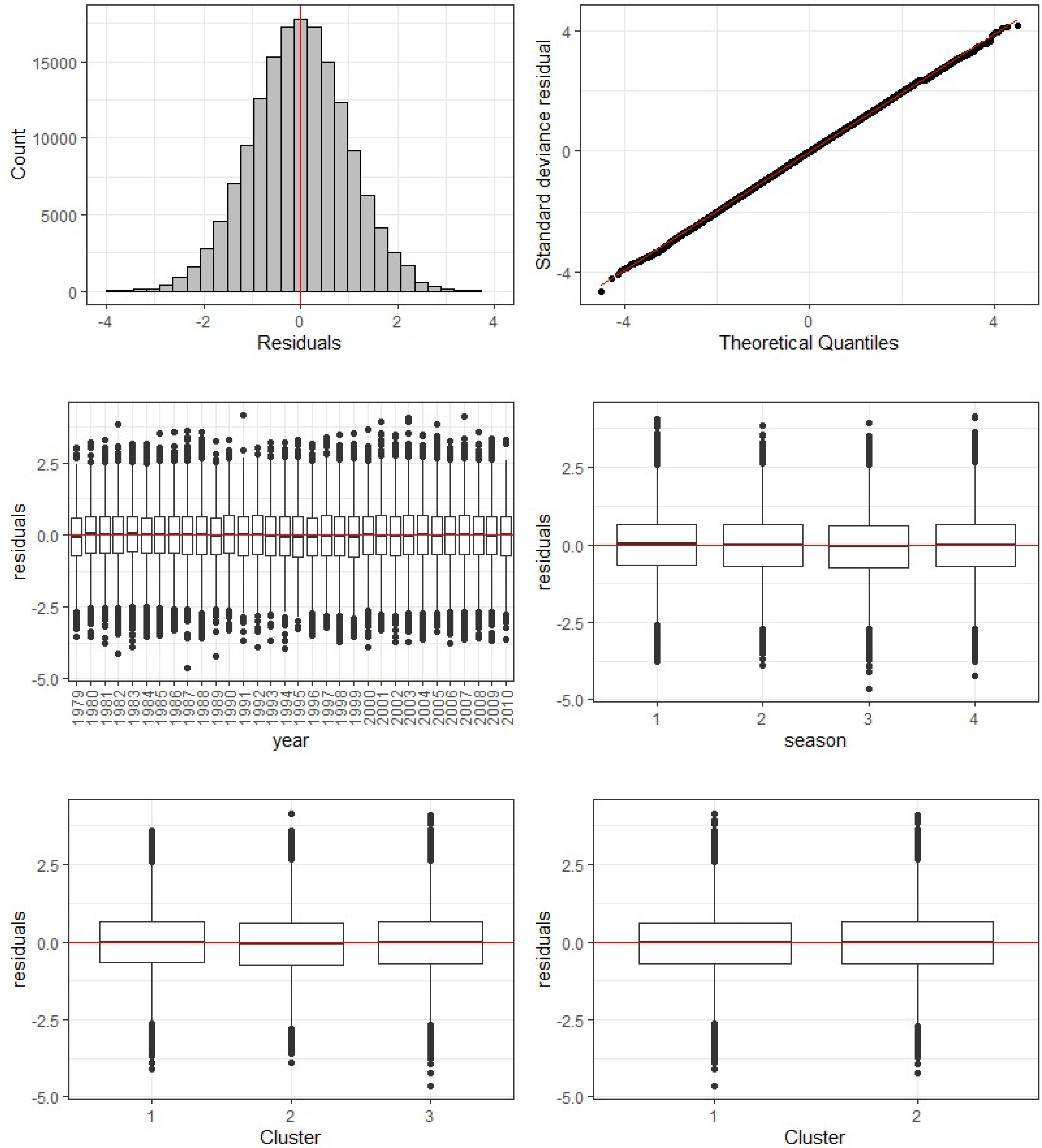

Fig. 7 Diagnostic plots of goodness-of-fit for the most parsimonious model (Model-6) for the former period (1979-2010).

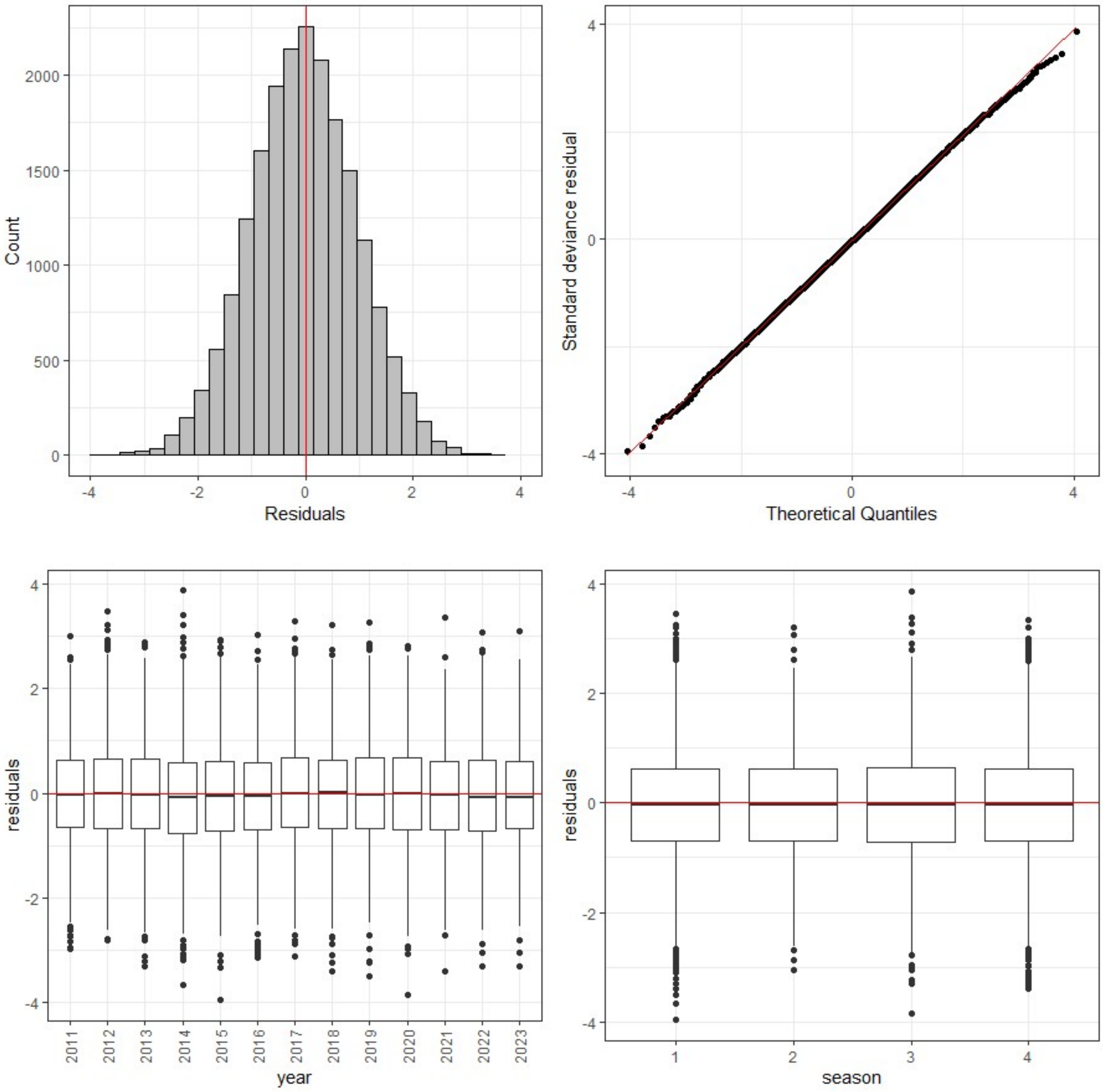

Fig. 8 Diagnostic plots of goodness-of-fit for the most parsimonious model (Model-4) for the latter period (2011-2023).

Fig. 9 Spatial distribution of log-scaled predicted CPUE for the former period (1979-2010). One hundred knots are given in the estimation of the standardized CPUE.

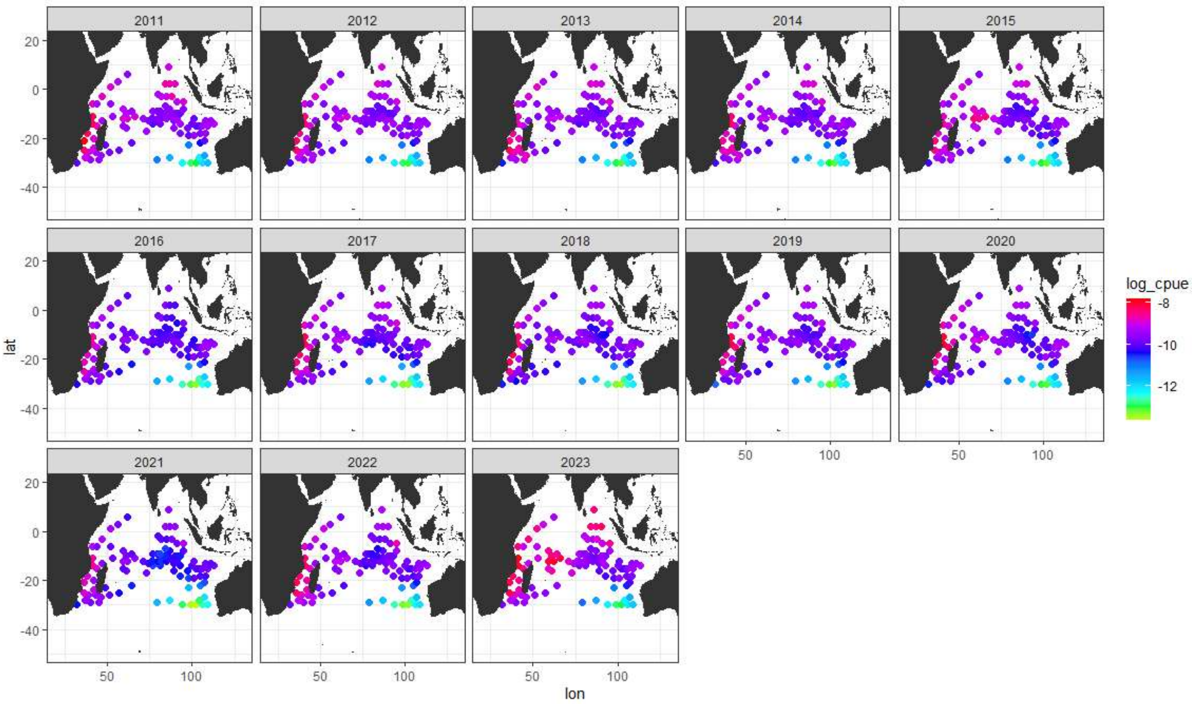

Fig. 10 Spatial distribution of log-scaled predicted CPUE for the latter period (2011-2023). One hundred knots are given in the estimation of the standardized CPUE.

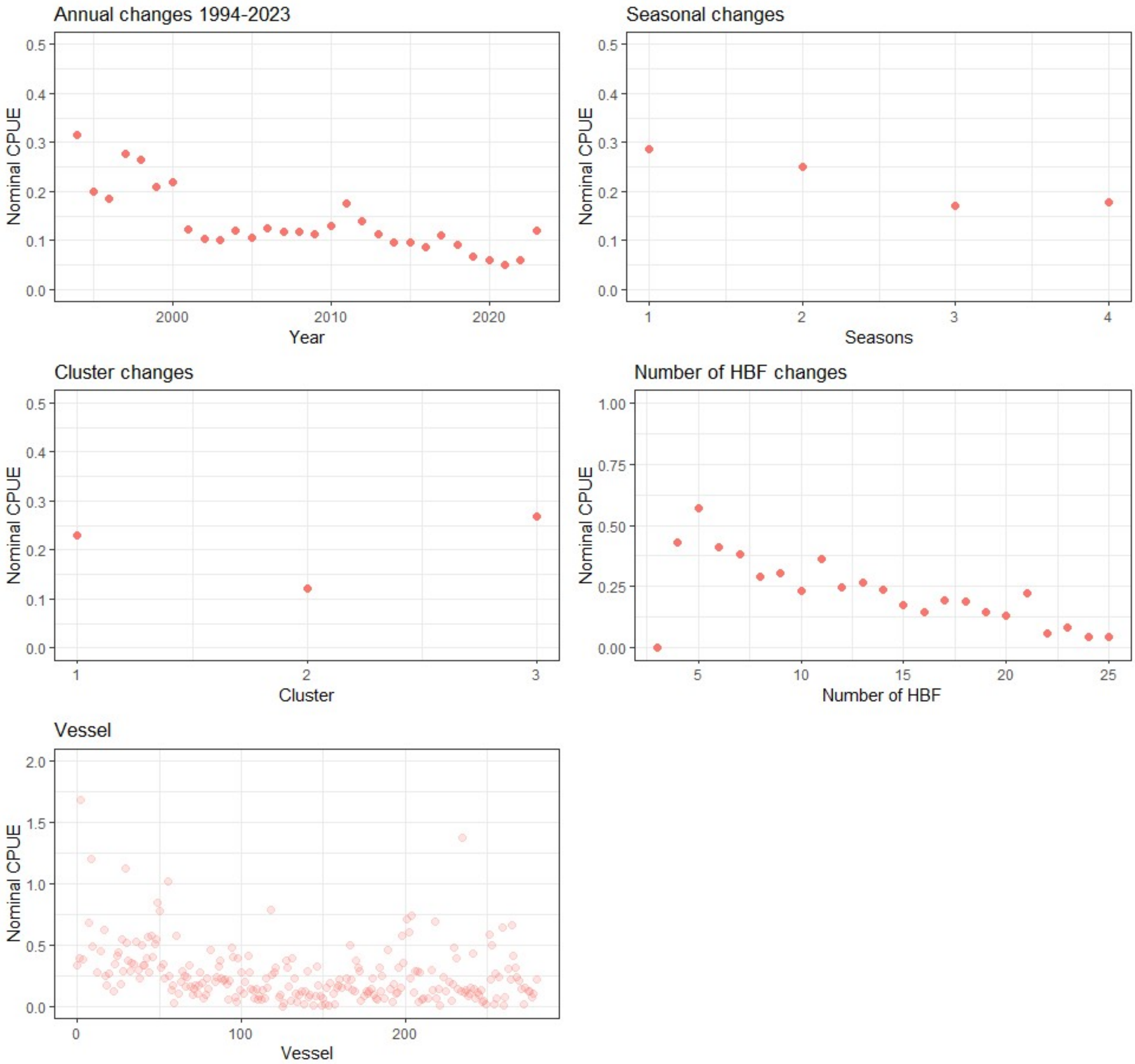

Fig. A1 Changes in nominal CPUE (per 1000 hooks) by year, season, targeting cluster, number of hooks between floats (HBF), and vessel for the filtered data of blue marlins in the Indian Ocean.

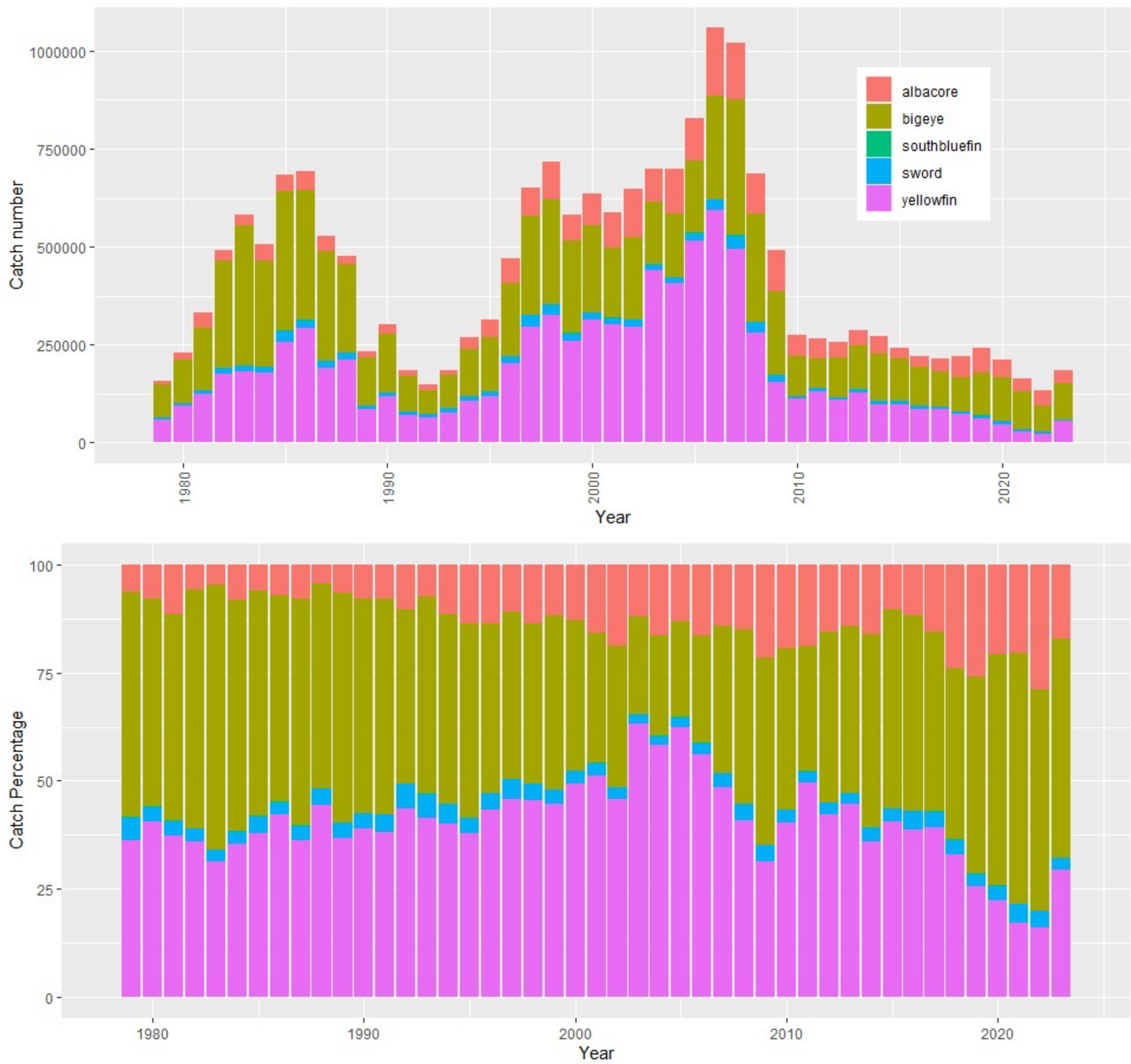

Fig. A2 Annual changes in the species composition of catch numbers (upper panel) and the proportion of catch numbers (lower panel) for tunas and tuna-like species caught by the Japanese longline fishery in the Indian Ocean from 1979 to 2023.

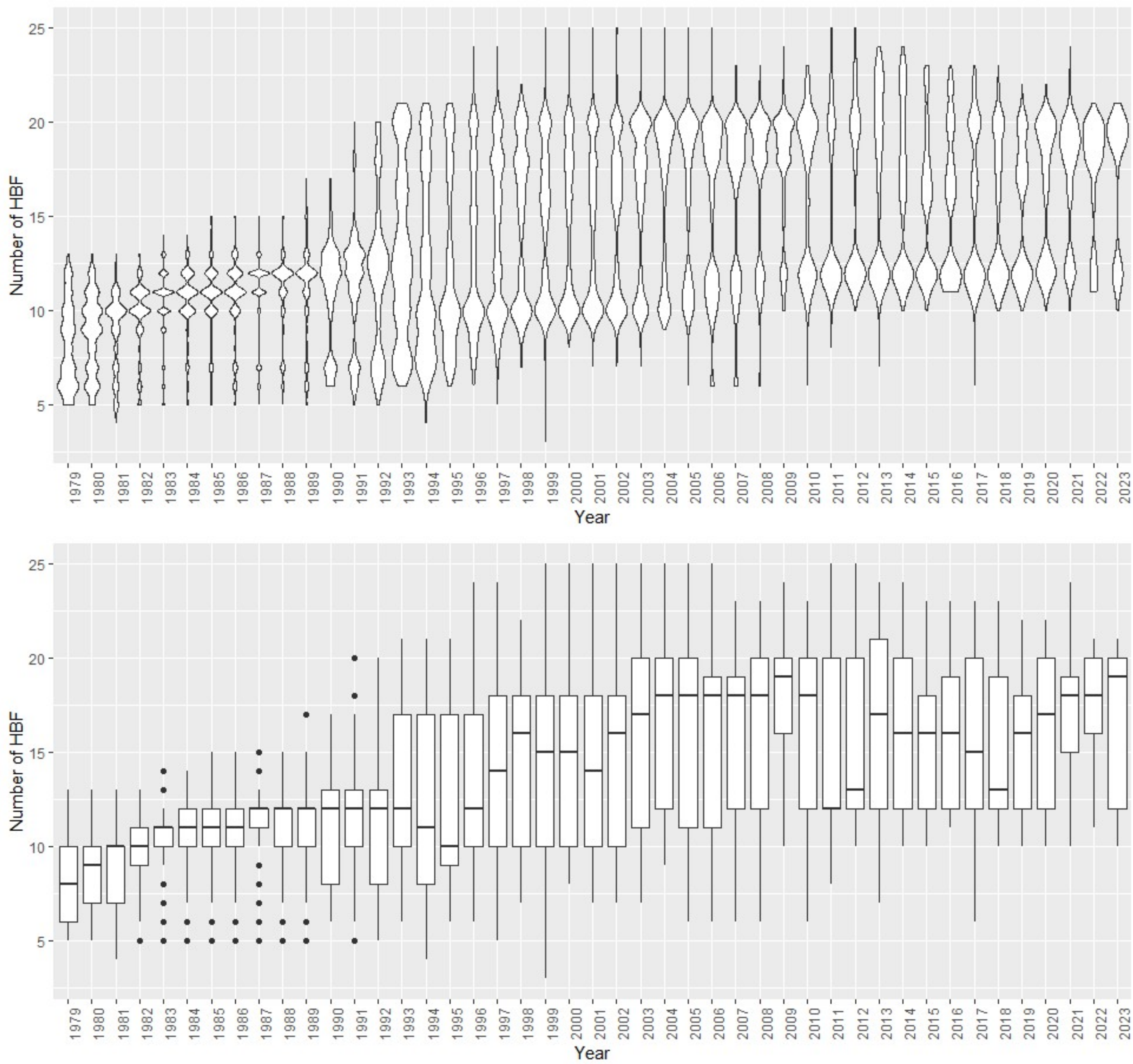

Fig. A3 Annual changes in the number of hooks between floats (HBF) (upper panel shows a violin plot, and lower panel shows a boxplot) used in the Indian Ocean.

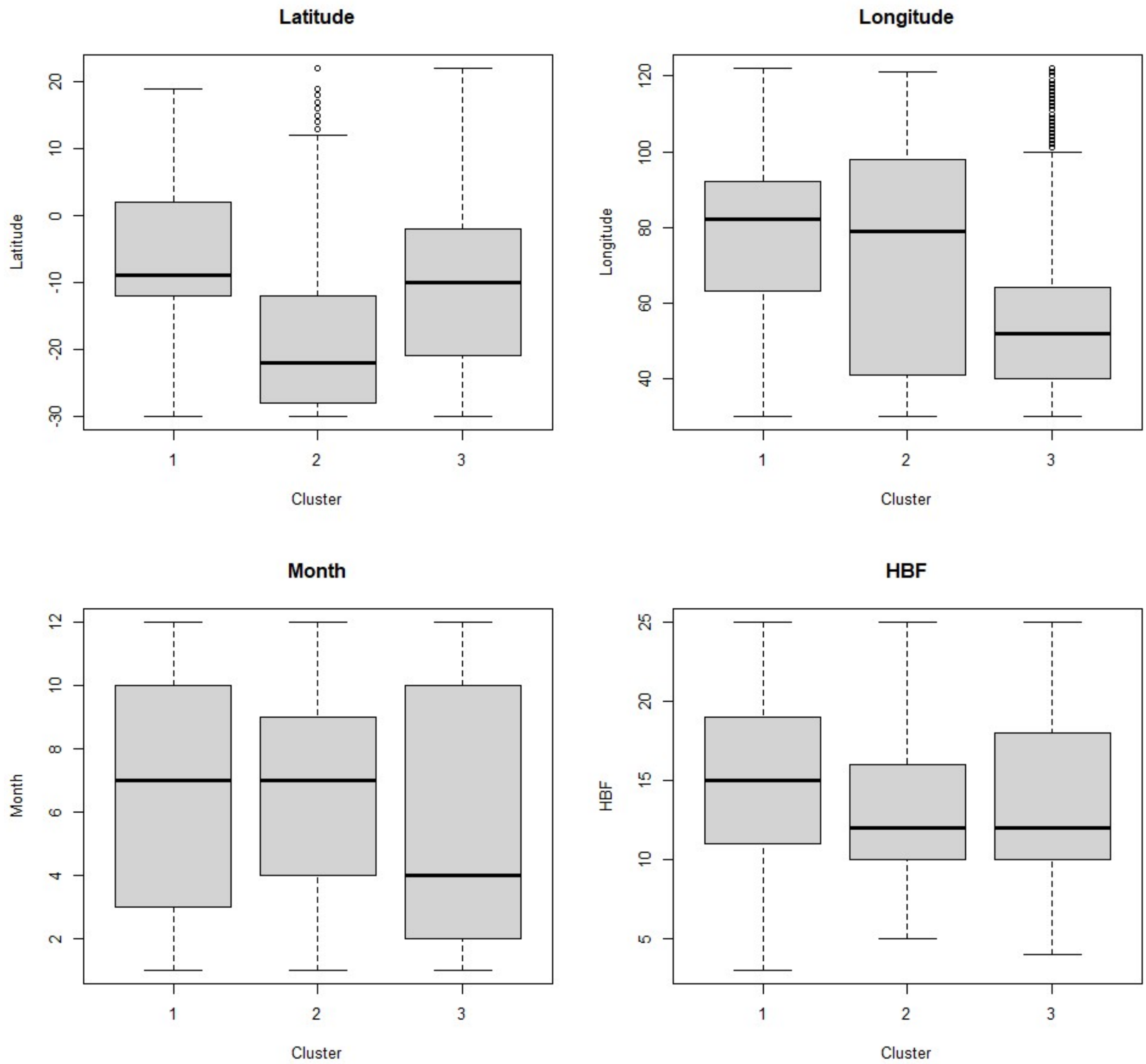

Fig. A4 Boxplots of latitude, longitude, month, and HBF for each cluster based on composition of three species (Yellowfin, bigeye tuna, and albacore). The thick line represents the median, and the upper and lower bounds of the box represent the third quartile and first quartile, respectively.

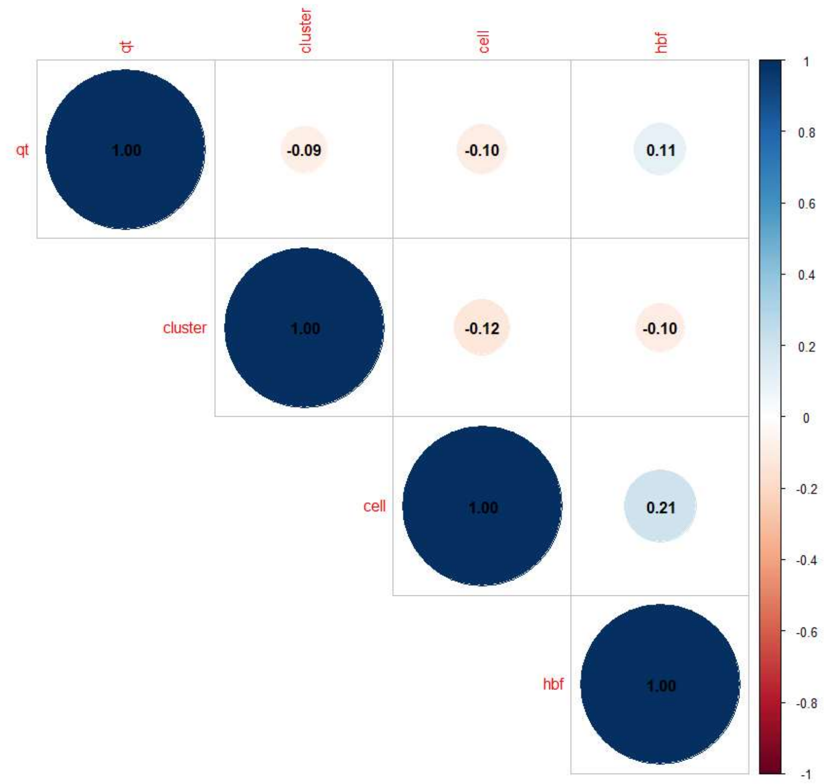

Fig. A5 Correlation among quarters, number of hooks between floats (HBF), cell (station), and cluster using filtered datasets in the Indian Ocean. This figure was created based on the data after filtering.

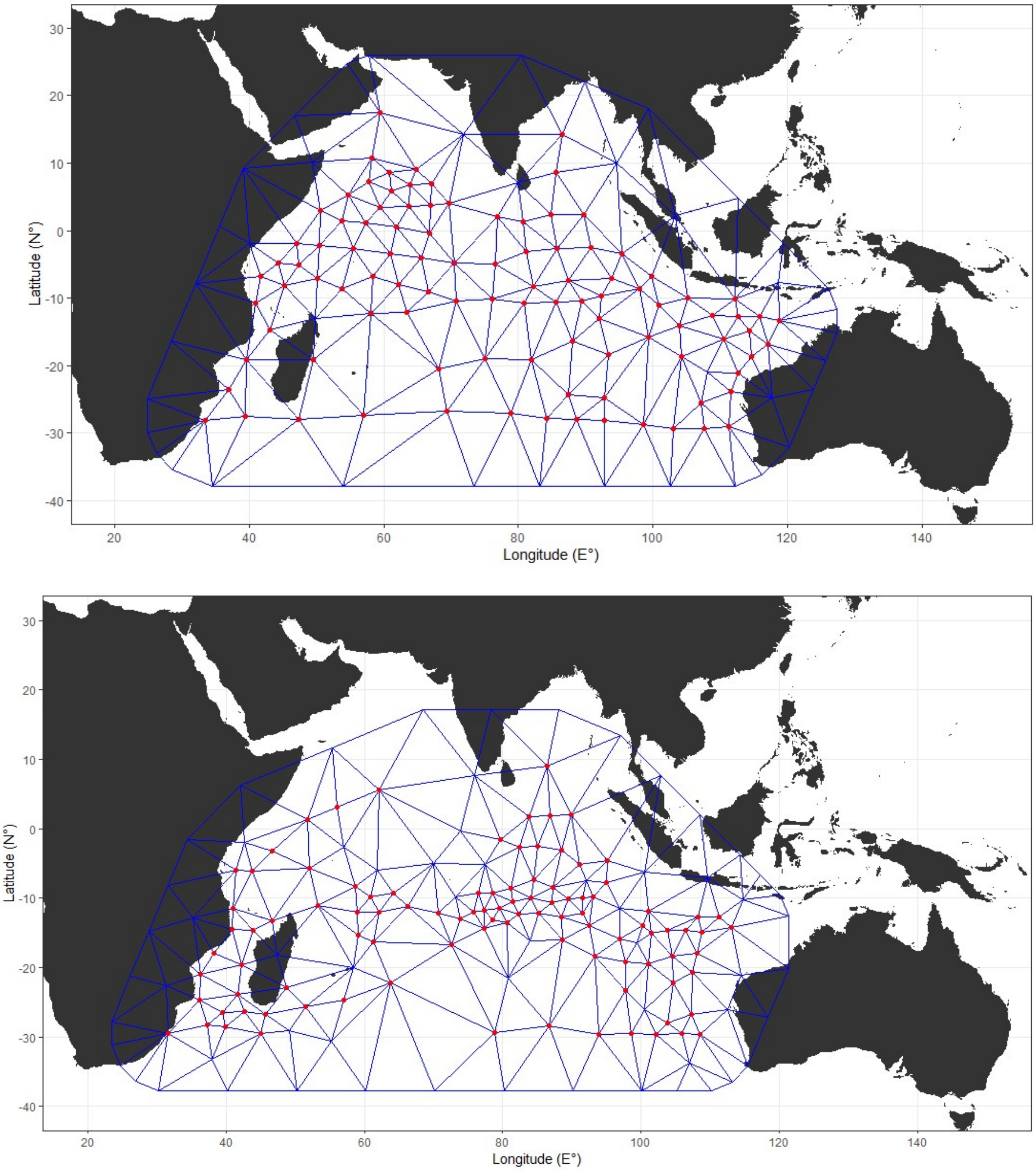

Fig. A6 Triangulation map used in the present analysis for the former period from 1979 to 2010 (upper panel) and latter period from 2011 to 2023 (lower panel). The red points denote one hundred knots.

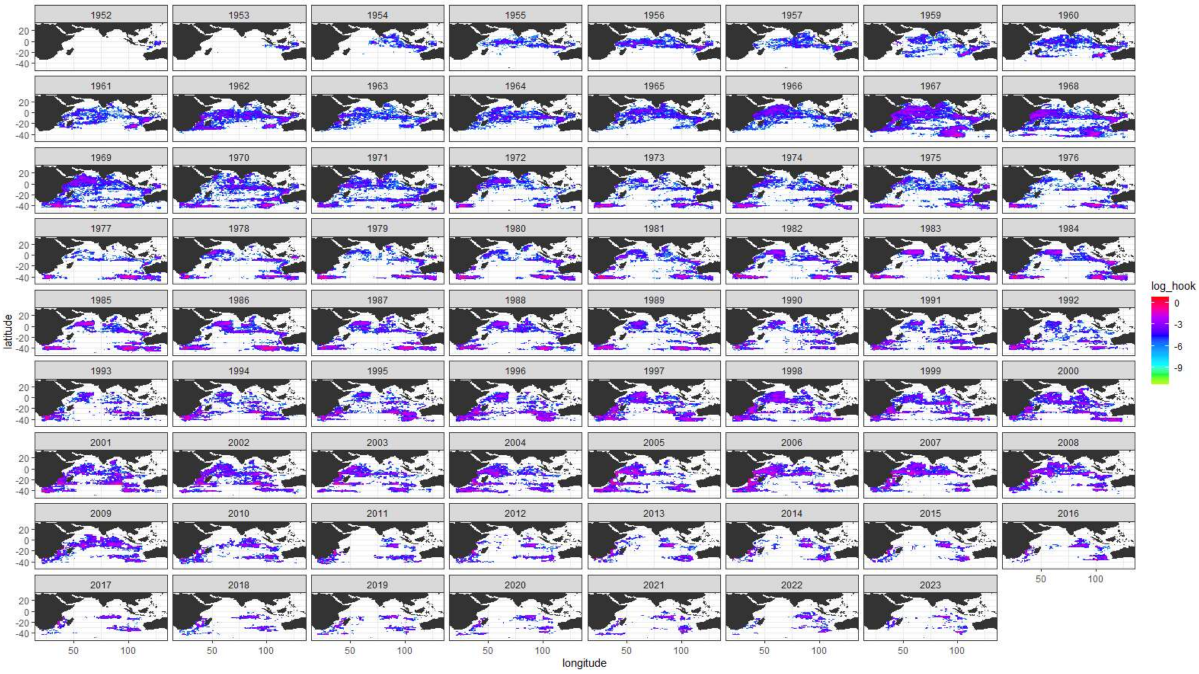

Fig. A7 Annual changes in the spatial maps of fishing effort (log scale of the total number of hooks) by Japanese tuna longline fleets in the Indian Ocean from 1952 to 2023.